Current Applied Physics 11 (2011) S333–S338

Contents lists available at ScienceDirect

Current Applied Physics

journal homepage: www.elsevier.com/locate/cap

Wind-power generators based on ZnO piezoelectric thin films on stainless steel substrates

Wei-Tsai Chang [a], Ying-Chung Chen [a], Re-Ching Lin [a], Chien-Chuan Cheng [b,*], Kuo-Sheng Kao [c], Yu-Chang Huang [a]

[a] Department of Electrical Engineering, National Sun Yat-Sen University, Kaohsiung, Taiwan, ROC
[b] Department of Electronic Engineering, De Lin Institute of Technology, Taipei, Taiwan, ROC
[c] Department of Computer and Communication, Shu-Te University, Kaohsiung, Taiwan, ROC

ARTICLE INFO

Article history:
Received 31 August 2010
Accepted 1 November 2010
Available online 5 November 2010

Keywords:
ZnO
Piezoelectric transducer
Power generator
Stainless steel substrate

ABSTRACT

This paper reports a novel means of integrating a high-performance ZnO piezoelectric transducer with a flexible stainless steel substrate (SUS304) to construct a wind-power generator. The stainless steel substrate has a higher Young's modulus than that of the PET substrate, and will behave the long-term stability under vibration. The transducer includes a ZnO piezoelectric film deposited on the stainless steel substrate at a temperature of 300 °C by an RF magnetron sputtering system. Scanning electron microscopy and X-ray diffraction of ZnO piezoelectric films reveal a rigid surface structure and a high c-axis-preferred orientation. To fabricate a transducer with a resonant frequency of 75 Hz for the natural winding, the cantilever length of 1 cm and a vibration area of 1 cm^2 are used, based on cantilever vibration theory. A mass loading of 0.57 g at the front-end of the cantilever is critical to increase the amplitude of vibration and the power generated by the piezoelectric transducer. The maximum open circuit voltage of the power generator is 10.5 V. After rectification and filtering through a 3.3 nF capacitor, the output power of the wind generators exhibited a specific power output of 1.0 $\mu W/cm^2$ with a load resistance of 5 MΩ.

Crown Copyright © 2010 Published by Elsevier B.V. All rights reserved.

1. Introduction

Various clean and green energy systems have been extensively developed and explored to help tackle the issue of energy shortage. Renewable sources of energy included hydroelectricity [1], wind [2–4], oceanic [5,6], solar [7–9] etc. Wind generation generally involves an aerodynamic blade system with synchronous permanent-magnet generators. Two common methods of wind generation are used in business. They are the use of wind generators that comprise a grid-connected power supply system and the use of a detached generator that also stores energy. Hydroelectric power plants are always built with the turbines, such as the Pelton turbine or the chain turbine.

Four forms of oceanic energy generation have been enthusiastically researched and developed. They include wave, tidal, ocean current-based and thermoelectric. Wave generator systems produce impulses as the amplitudes of ocean waves fluctuate. The output power of the tidal generator is produced from the potential energy and kinetic energy of the tidal current. An ocean current power plant is analogous to a hydroelectric power plant. The thermoelectric generator exploits deep sea water at different temperatures to drive the turbine system.

Solar energy refers the photovoltaic effect and thermal power generation. However, a solar energy system must be installed in an area with sufficient sunlight. Solar cells are expensive because of shortages of the materials from which they are fabricated.

Of the aforementioned sources of renewable energy, wind power is most prevalent. Several transducer technologies have been proposed for use in recyclable energy systems based on wind. They include electromagnetic [10], electrostatic [11], and piezoelectric [12,13] transducers. A commercial wind-power generator exploits the traditional electromagnetic effect. However, it generally requires a large operating spaces, complex instrumentations, and ongoing management of facilities, which are expensive. The electrostatic generator exploits Faraday's law and a variable capacitor to generate electric power. The volume of an electrostatic generator mechanism is enormous, and so it does not economically viable. Hence, several scholars have examined piezoelectric power generators, focusing mainly on the piezoelectric material (Pb, Zr)TiO_3 (PZT) [14,15].

* Corresponding author. Tel.: +886 2 22733567x157.
E-mail address: chengccc@dlit.edu.tw (C.-C. Cheng).

1567-1739/$ – see front matter Crown Copyright © 2010 Published by Elsevier B.V. All rights reserved.
doi:10.1016/j.cap.2010.11.007

Table 1
The properties of stainless steel substrates (SUS304).

Density (g/m^3)	7.86
Young's Modulus (GPa)	125.9
Thickness (μm)	50
Coefficient of thermal expansion (ppm/°C)	17.3
Tg (°C)	>1300

Table 2
Deposition parameters of ZnO thin films.

Target	Zn (99.995%)
Substrate-to-target distance (mm)	50
Base pressure (Torr)	2×10^{-6}
Substrate temperature (°C)	R.T., 100 °C, 200 °C, 300 °C, 400 °C
RF power (W)	50, 75, 100, 125, 150
Sputtering pressure (mTorr)	3, 9, 15, 21, 27
O_2/O_2+Ar	60%

However, the use of piezoelectric PZT devices is illegal because it causes serious environmental pollution. Therefore, ZnO-based micro-generators have been developed. They require a small working spaces; have a low operating frequency; are environmentally-friendly; exhibit long-term stability and can be used at low cost characteristics in clean energy applications. This report develops wind generators based on ZnO transducers that are integrated with stainless steel substrate (SUS304). In this study, flexible SUS304 is used as the bottom electrode in wind generator because of its flexibility and conductivity. SUS304 has such excellent properties, as heat-tolerance, anti-corrosion, wear resistance and mechanical strength.

This study will investigate the influences of sputtering parameters on the performance of ZnO-based generators to optimize the fabrication processes. The mechanical properties of ZnO thin films were analyzed using a nano-indenter and a nano-scratch tester. Finally, the electrical performance of ZnO-based generators is examined using a vibration testing system. The electrical properties

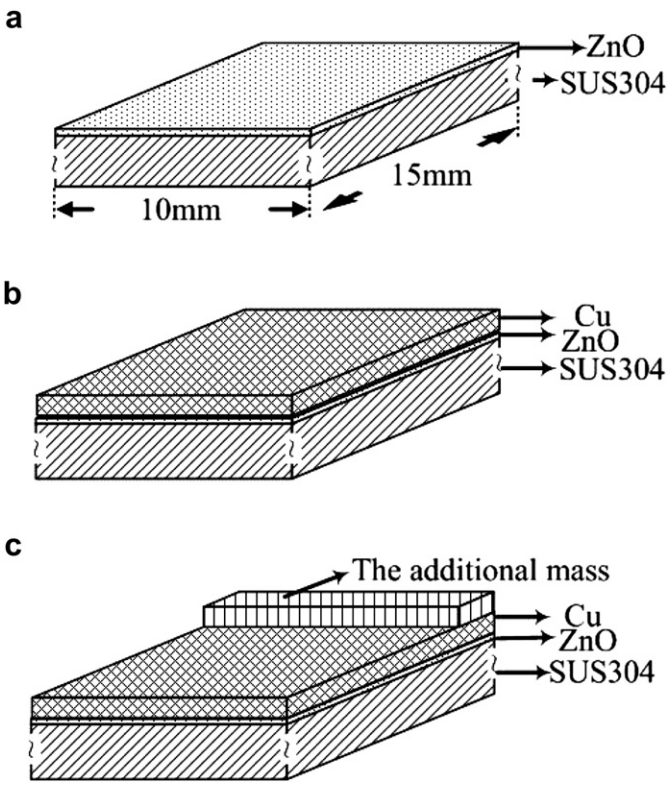

Fig. 1. The fabrication processes for the transducer device.

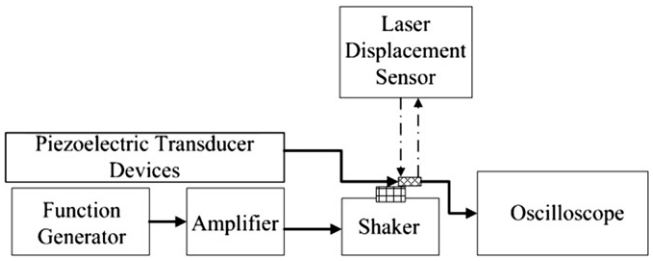

Fig. 2. The measurement system for the transducer device.

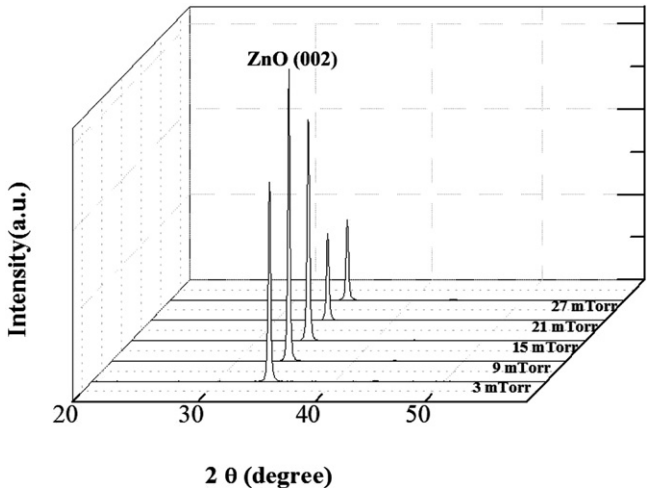

Fig. 3. The θ-2θ X-ray scans of the ZnO thin films deposited with various sputtering pressures.

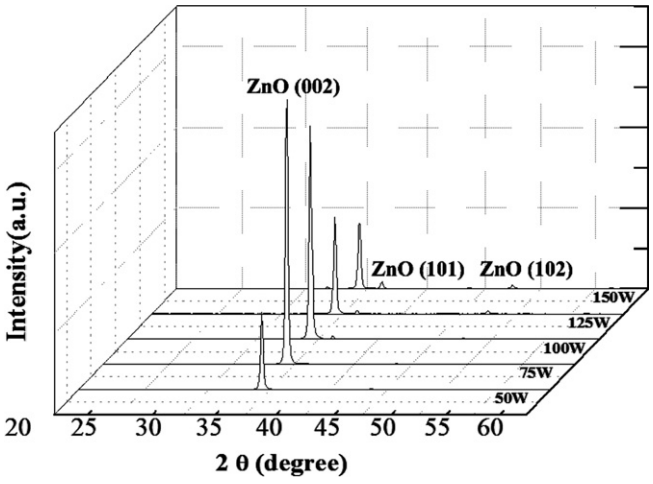

Fig. 4. The θ-2θ X-ray scans of the ZnO thin films deposited with various RF powers.

considered in the evaluation of generator performance included the AC output voltage, the signal with loading and the signal after rectification and filtering.

2. Experimental details

In this study, the reactive radio-frequency (RF) magnetron sputtering method was employed to deposit ZnO piezoelectric thin films. The sputtering system was evacuated to a base pressure of 2×10^6 Torr using a diffusion pump to achieve the required deposition conditions. The SUS304 substrates with 50 μm thickness were adopted as flexible substrates and bottom electrodes in wind generators. Table 1 presents the properties of stainless steel substrates (SUS304). After the cleaning of substrates by standard spotless process, the ZnO piezoelectric thin film was deposited by RF sputtering with heating. Table 2 shows in detail the sputtering

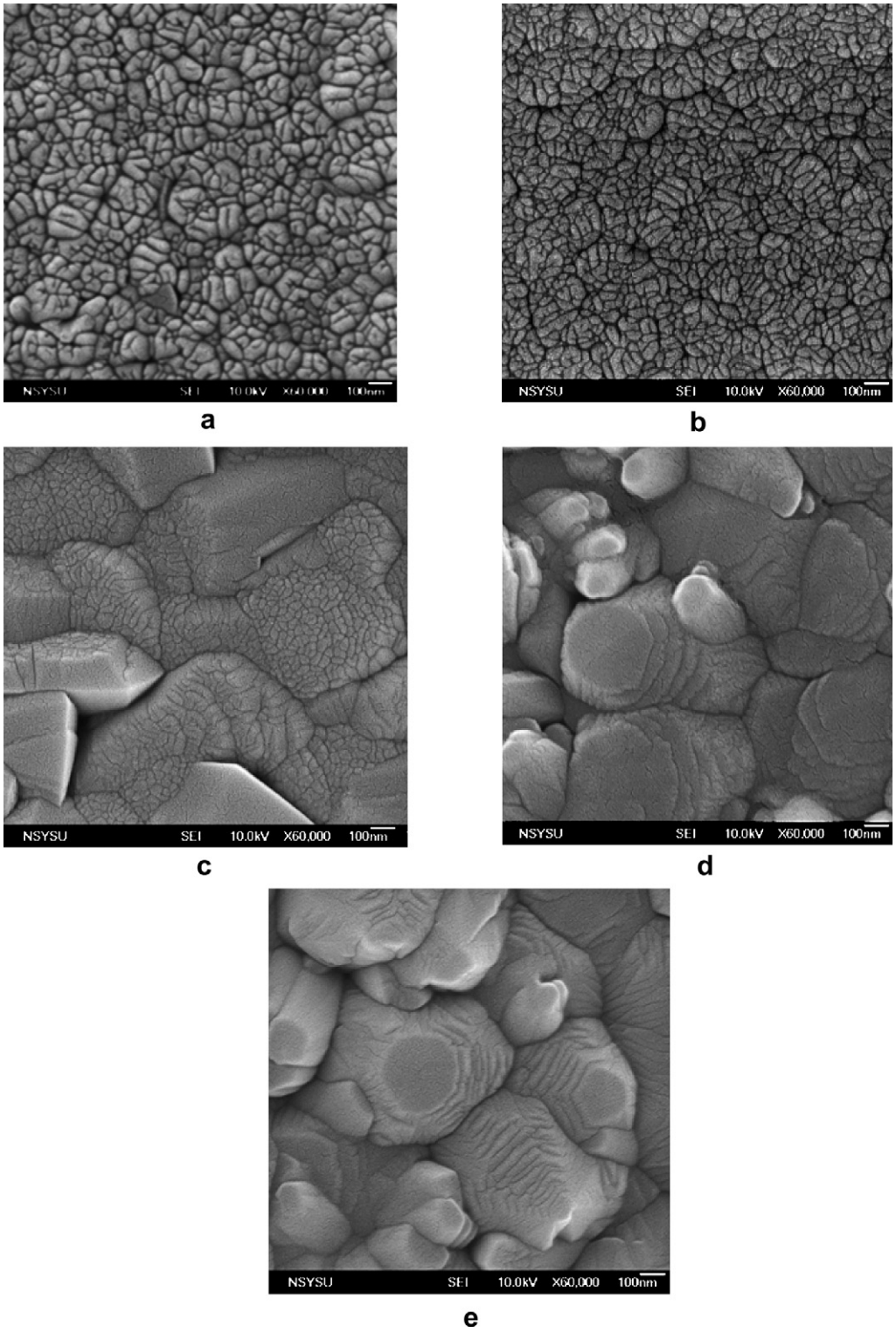

Fig. 5. The surface morphology of the ZnO thin films deposited with various RF powers: (a) 50 W, (b) 75 W, (c) 100 W, (d) 125 W, and (e) 150 W.

conditions of preparing c-axis-oriented piezoelectric ZnO thin films. After the ZnO/SUS304 structure was formed, a copper (Cu) layer was attached to the ZnO/SUS304 substrate as the top electrode in a piezoelectric transducer, because it has a low resistivity and is inexpensive. Finally, the electrical properties of the transducers (Cu/ZnO/SUS304) were measured using a vibration testing system. To increase the amplitude of vibration of the transducers to facilitate measurement, an additional mass loading of 0.57 g on the cantilever was attached to the transducer. Fig. 1 displays the fabrication of the device.

The preferred orientation and crystalline properties of the ZnO films were determined by X-ray diffraction (XRD) using an SHIMADZU XRD-6000 with CuKα radiation. The cross-sectional morphologies of the ZnO films were observed by scanning electron microscopy (SEM) (Philips XL40 FESEM). The thicknesses of the ZnO films were measured by reflectance spectroscopy (RS) (Filmetrics F20), and their mechanical properties were measured using a nano-indenter (MTS NanoIndenter G200). Fig. 2 presents the system for measuring the electrical properties of the ZnO transducers, which is a permanent-magnet vibration testing system (B&K-LDS V201-PA25E). The system included a laser displacement sensor (MEL M72L/4) for measuring the amplitude of vibration.

3. Results and discussion

3.1. Structural and morphological properties of piezoelectric ZnO thin films

To optimize the piezoelectric characteristics of RF-sputtered ZnO thin films for use in wind-power generators, the deposition parameters were investigated. The ideal physical properties of piezoelectric films for use in piezoelectric transducer applications are a strong c-axis orientation and a uniform surface structure. In this study, RF power, sputtering pressure and substrate temperature were varied to optimize these characteristics. At first, the sputtering pressure was controlled to achieve the optimal ZnO layer. The heating process was reported to improve the piezoelectric properties of ZnO thin films. Therefore, in this study, the sputtering pressure was varied and the substrate temperature was set at 300 °C to investigate the effect of the pressure on ZnO thin films. As shown in Fig. 3, a sputtering pressure of 9 mTorr resulted in the optimal crystallization and a high electromechanical coupling coefficient. Then, the RF power was controlled and the substrate temperature was set at 300 °C to investigate the influence of RF power on ZnO thin films. The XRD patterns in Fig. 4 reveal that ZnO thin films deposited at 75 W yielded a sharp (002) peak with small full width at half maximum (FWHM). Additionally, as shown in Fig. 5, the grain size in the ZnO thin films increased with the increase of RF power, because of the bombardment by the zinc irons and the thermal effect. Therefore, the RF power was fixed at 75 W to produce a highly textured structure of ZnO thin films.

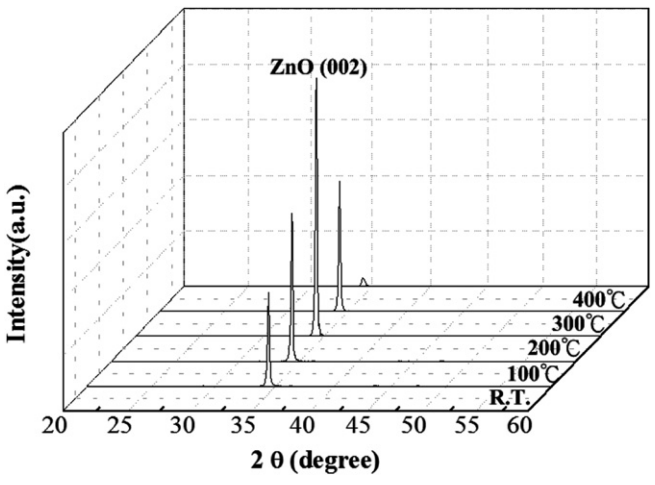

Fig. 6. The θ-2θ X-ray scans of the ZnO thin films deposited with various substrate temperatures.

Table 3
The internal resistance of ZnO thin films with various substrate temperatures.

Substrate temperatures	R.T.	100 °C	200 °C	300 °C	400 °C
R_{ZnO} (MΩ)	1.25	2.92	5.47	5.10	NA

Fig. 6 reveals the variation of the XRD patterns of the ZnO thin films that were deposited on the SUS304 substrates with various substrate temperatures. A sharp (002) peak with narrow FWHM is obtained at the substrate temperatures from room temperature (R.T.) to 300 °C. A stronger XRD intensity indicates that the ZnO thin film has a higher electromechanical coupling coefficient of piezoelectricity. The diffraction angle of ZnO thin films matches that of the standard ZnO film. However, the internal resistance of the ZnO thin films increased with the increase of the piezoelectricity, as presented in Table 3. In order to determine the optimal substrate temperature to obtain the well piezoelectricity and the low internal resistance, four kinds of transducers were performed with ZnO thin films deposited at R.T., 100 °C, 200 °C and 300 °C, respectively. The open-circuited output voltages (V_{p-p}) of the four transducers were measured, as shown in Table 4. The output voltage and the loaded voltage in transducers 1, 2 and 3 are lower than those in transducer 4. So, in this study, the substrate temperature of 300 °C was adopted to ensure the output voltage and high electromechanical coupling coefficient of piezoelectricity.

Finally, the optimal substrate temperature of 300 °C, RF power of 75 W and sputtering pressure of 9 mTorr were used to deposit piezoelectric ZnO films with a smooth surface, uniform grain size and strongly c-axis-orientated crystallization, as shown in Fig. 7. The surface morphologies of ZnO films deposited on the SUS304 substrates appeared dense, had smooth surfaces and strongly textured columnar structures. Hexagonal crystals, such as ZnO, are believed to exhibit piezoelectricity of unity with a (002)-preferring orientation.

3.2. Analysis of adhesion of ZnO thin films with SUS304 substrate

In this investigation, a nano-indenter and a nano-scratch tester were applied to elucidate the mechanical properties of ZnO thin films. Table 5 presents the conditions for measuring the mechanical properties of ZnO thin films. Fig. 8 shows the optical microscopic (OM) images before and after the test. The results show that the ZnO/SUS304 structure has several favorable prosperities, such as high compressive strength, high fracture strength and the absence of any breakage phenomenon. Fig. 9 presents the scratch depth of the ZnO thin film deposited on the SUS304 substrates with various applied

Table 4
The output voltages of four transducers.

Transducer No.	Substrate Temperature	V_{p-p} (V)
Transducer 1	R.T.	1.2
Transducer 2	100 °C	1.52
Transducer 3	200 °C	2.68
Transducer 4	300 °C	7.76

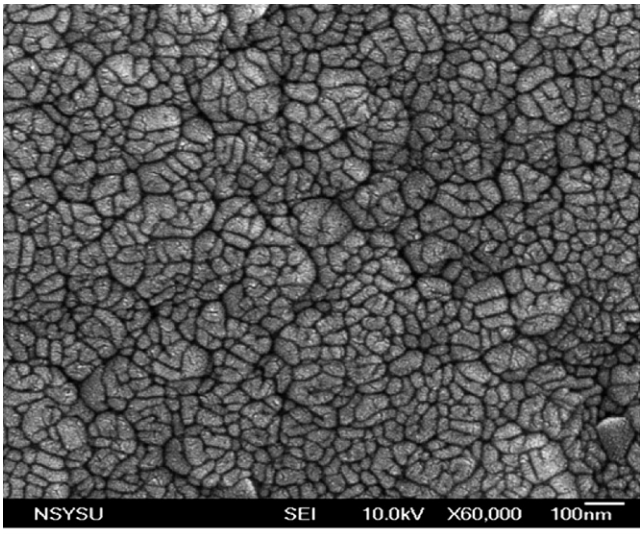

Fig. 7. Surface and cross-section morphology of ZnO thin films deposited with the optimized parameter.

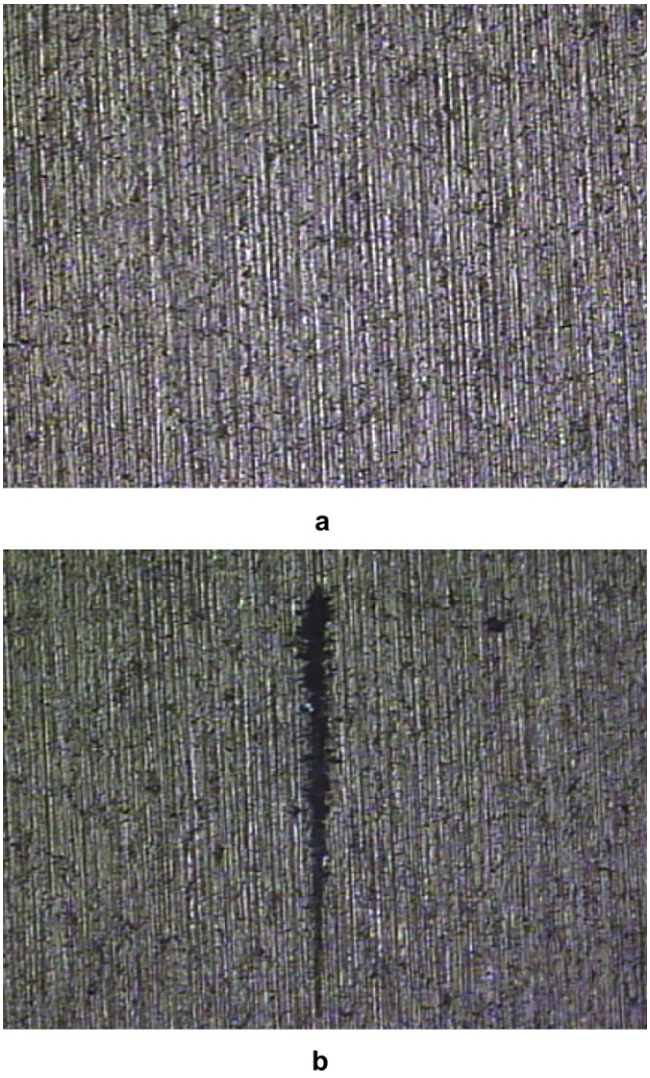

Fig. 8. The optical microscopy (OM) drawing of the ZnO thin films: (a) the reset condition, (b) after the nano-indenter and nano-scratch tester.

stresses. Point A in Fig. 9 indicates that the ZnO/SUS304 structure endured 500 mN of applied stress without any change to the shape of the surface. Point B in Fig. 9 reveals that the end point and the starting point are coincidental, so no extrusion phenomenon occurs. Therefore, the ZnO/SUS304–based structure is highly stable and will sustain long-term vibration in the nature environment.

3.3. Electrical properties of generators

According to the investigation [16], the excitation frequency and the amplitude of vibration critically influence the output voltage of

Table 5
The parameters of the nano-indenter and nano-scratch tester.

Scratch Length (μm)	500
Scratch Velocity (nm/s)	100
Starting scratch load (mN)	1
Maximum scratch load (mN)	520
Allowable drift rate (nm/s)	1
Profiling acquisition rate (Hz)	20
Load applied during profiling (μN)	100

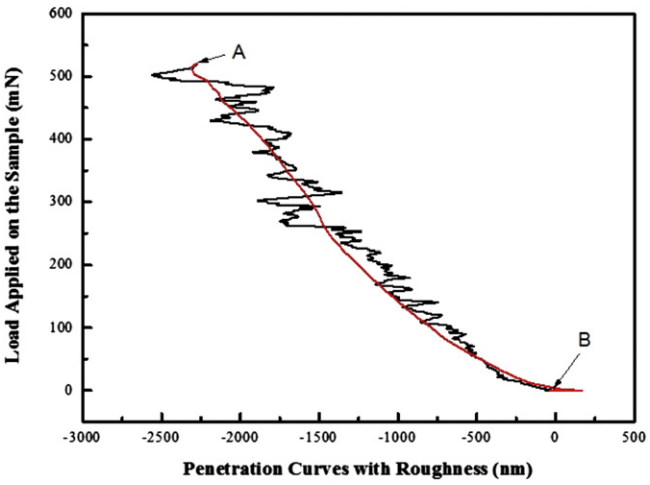

Fig. 9. The indentation depth variations of the ZnO thin films deposited on the SUS304 substrates with various extra stresses.

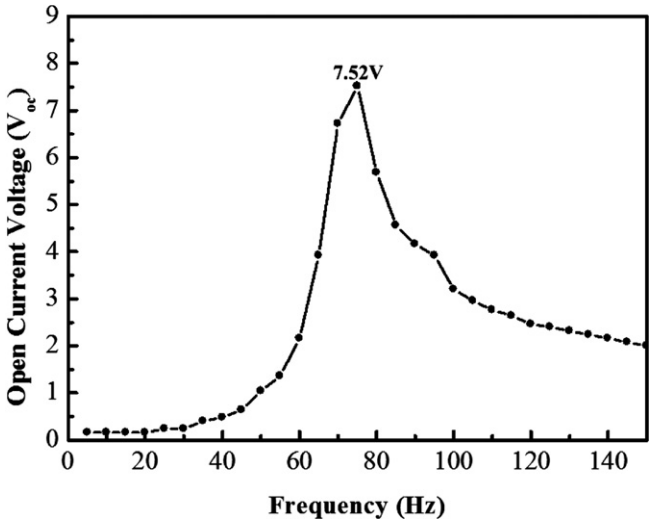

Fig. 10. The variation of open circuit voltage (V_{oc}) with various excited frequencies.

a generator. Fig. 10 plots the variation of open circuit voltage (V_{oc}) with excitation frequencies, in which a maximum V_{oc} of 7.52 V was achieved at an excitation frequency of 75 Hz. Clearly, the ZnO-based generator in this study is suitable for low frequency application. Fig. 11 plots the variations in V_{oc} with the amplitude of vibration. The maximum V_{oc} of 10.5 V is reached at the vibration amplitude of 1.19 mm and vibration frequency of 75 Hz.

The piezoelectric transducer can be characterized as high-voltage with a low current output. For practical applications, the ZnO-based transducers were rectified by a bridge circuit using four Schottky diodes (1N5711) and filtered with a capacitor of 33 nF. In order to investigate the maximum power transport, a load resistor of 5 MΩ was chosen because of the ~5 MΩ internal resistance of the transducers, as shown in Table 3. Fig. 12 shows the open circuit voltage, the output voltage rectified by the bridge circuit, the DC voltage after filtered with the 33 nF capacitor and the DC voltage after filtered and 5 MΩ loaded using the optimized transducer with the vibration amplitude of 1.19 mm and vibration frequency of 75 Hz. The maximum DC output voltage with loading was 2.24 V and the maximum output power was 1.0 μW/cm^2.

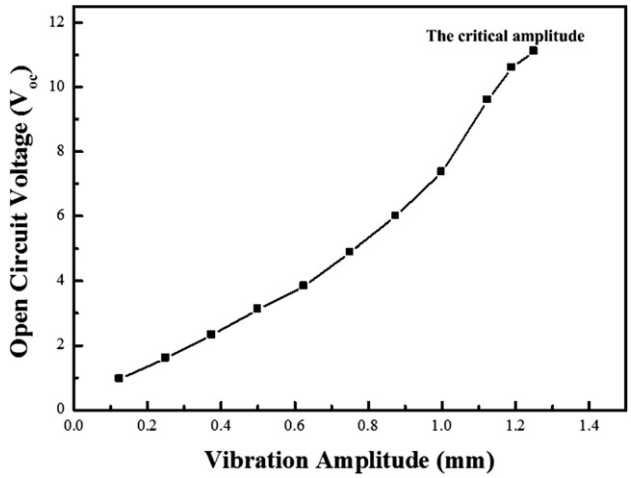

Fig. 11. The variations of V_{oc} with various vibration amplitudes.

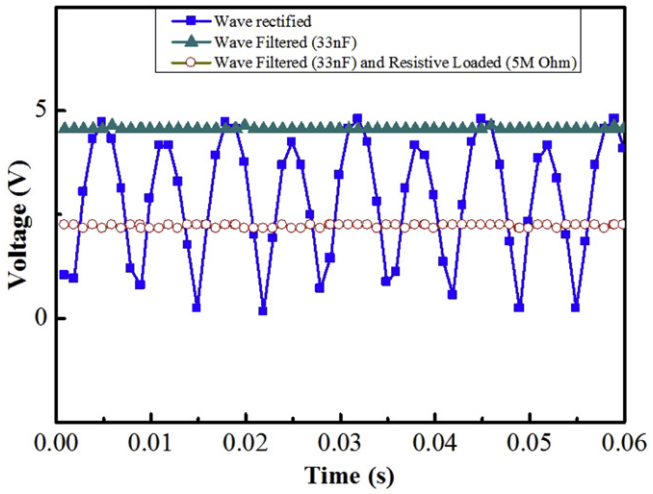

Fig. 12. The waves forms of maximum DC output voltages of optimized piezoelectric transducer after rectified, filtered and resistive loaded.

4. Conclusion

In this study, a wind-power generator based on a ZnO/SUS304 layered piezoelectric transducer was fabricated. Its performance was explored. The c-axis-oriented ZnO thin films were effectively deposited on flexible stainless steel substrates with particular sputtering parameters. The ZnO film had not only a uniform grain size and smooth surface, but also a strong c-axis orientation and a columnar structure. The strong crystalline properties of thin film contributed substantially to the desired piezoelectricity of the piezoelectric transducer. The ZnO/SUS304 wind-power generator provided an output power of 1.0 μW/cm^2.

Acknowledgement

The authors would like to thank the National Science Council of the Republic of China, Taiwan, for financially supporting this research under contracts Nos. NSC97-2221-E-110-011-MY2, NSC98-2221-E-237-002 and NSC99-2221-E-110-041-MY2.

References

[1] M.M. Kuraica, B.M. Obradovic, D. Manojlovic, D.R. Ostojic, J. Puric, Vacuum 73 (2004) 705–708.
[2] T.K.A. Brekken, N.K.S. Mohan, IEEE Transaction on Energy Conversion 22 (2007) 129–135.
[3] E. Koutroulis, D. Kolokotsa, A. Potirakis, K. Kalaitzakis, Solar Energy 80 (2006) 1072–1088.
[4] R. Pallabazzer, Solar Energy 55 (1995) 49–59.
[5] L.S. Blunden, A.S. Bahaj, Proceedings of the Institution of Mechanical Engineers, Part A: Journal of Power and Energy 221 (2007) 137–146.
[6] J. Behrens, N. Rakowsky, W. Hiller, D. Handorf, M. Lauter, J. Papke, K. Dethloff, Ocean Model 10 (2005) 171–183.
[7] B. O'Regan, M. Gratzel, Nature 353 (1991) 737–739.
[8] M.A. Green, K. Emery, D.L. King, Y. Hishikawa, W. Warta, Progress in Photovoltaics: Research and Applications 15 (2007) 35–40.
[9] J. Britt, C. Ferekides, Applied Physics Letters 62 (1993) 2851–2852.
[10] T.L. Smith, J.D. Ferry, F.W. Schremp, Japanese Journal of Applied Physics 20 (1949) 144–153.
[11] M.J. Anderson, J.A. Hill, C.M. Fortunko, N.S. Dogan, R.D. Moore, Journal of the Acoustical Society of America 97 (1995) 262–272.
[12] S.J. Jeong, M.S. Kim, J.S. Song, H. Lee, Sensors and Actuators A 148 (2008) 158–167.
[13] J.Q. Liu, H.B. Fang, Z.Y. Xu, X.H. Mao, X.C. Shen, D. Chen, H. Liao, B.C. Cai, Microelectronics Journal 39 (2008) 802–806.
[14] H.B. Fang, J.Q. Liu, Z.Y. Xu, L. Dong, L. Wang, D. Chen, B.C. Caia, Y. Liub, Microelectronics Journal 37 (2006) 1280–1284.
[15] P.G. Jones, S.P. Beeby, N.M. White, IEE Proceedings. Science, Measurement and Technology 148 (2001) 68–72.
[16] L.Y. Taha, B.Y. Majlis, A. Al Ali, IEEE International Conference on Semiconductor Electronics, ICSE (2006) 294–298.